



Mapping Groundwater-Dependent Ecosystems in the Urumqi River and Chai Wo-pu Basins Using Geospatial Technologies and Field Data

Zhihao Ye^{1,2}, Qiang Zhou¹, Mingxia Zheng¹, Xiaoyu Zhang¹, Xin Zhou^{1*}, Liansheng He^{1*}, Longhao Huang^{1,2} and Rui Meng¹

¹ Institute of Aquatic Ecology and Environment, Chinese Research Academy of Environmental Sciences, Beijing, 100020, P. R. China

² College of River and Ocean Engineering, Chongqing Jiaotong University, Chongqing, 400000, P. R. China

Correspondence to: Xin Zhou (zhouxin_1991@126.com)

Abstract: Groundwater-Dependent Ecosystems (GDEs) are widely distributed in arid and semi-arid regions and serve as critical ecological safety barriers. However, the precise identification and mapping of GDEs has long posed a challenge for researchers, as the integration of geospatial technologies and field measurement techniques has remained insufficient. This study selected the final year of a prolonged drought period and the current year for analysis. Key indicators, including vegetation cover (FVC), the difference between evapotranspiration and precipitation (ET-P), Terrain Wetness Index (TWI) and the vegetation groundwater uptake index (VGUI), were employed. The K-means clustering algorithm was applied for classification, and spatial overlay analysis was performed in the Urumqi River and Chai Wo-pu Basin in Xinjiang, China, to assess the spatial distribution and temporal variations of GDEs. Additionally, the results were validated through the integration of wetland distribution and field investigations. The findings indicate that areas classified as "likely" or "very likely" GDEs are predominantly concentrated around Dongdao Haizi, Chai Wo-pu Lake, salt lakes, and adjacent regions, covering 45.4% of the potential area. Over time, the area classified as "unlikely" and "highly unlikely" for GDEs shows an increasing trend. By introducing field data of the VGUI, the study eliminates the interference from factors such as human irrigation in the identification of GDEs in typical areas, achieving refined mapping. This work provides valuable insights for the precise identification of GDEs in arid and semi-arid regions.

Keywords: Groundwater-Dependent Ecosystems; Urumqi River and Chai Wo-pu Basin; Integrated Mapping; Geospatial Technologies; Field Validation

Introduction

Water resources are a critical factor influencing human well-being. With population growth, accelerated social development, and the intensification of climate change due to global warming and prolonged droughts, water scarcity has become a major global challenge (Huang et al., 2019). Groundwater constitutes a key component of Earth's liquid freshwater, accounting for 96% of the total (Duran-Llacer et al., 2022). Groundwater plays a significant role as both a resource and an ecological buffer,



35 serving not only as a crucial source of drinking water and irrigation but also mitigating the effects of climate change. Additionally, it provides part or all of the water necessary for the survival of plants and animals(Howard et al., 2023). In arid and semi-arid regions, groundwater is the primary water source for certain plants and plays a crucial role in local human societies and natural ecosystems(Mamattursun et al., 2022a). However, groundwater resources are under increasing pressure from the combined effects of global climate change and human activities, such as over-extraction, leading to a range of ecological challenges(Eamus et al., 2006). Identifying groundwater-dependent ecosystems (GDEs) and assessing their dependence on groundwater can reveal the eco-hydrological factors sensitive to groundwater changes and associated ecological thresholds, thus helping to understand the evolution mechanisms of GDEs (Gibso et al., 2022), which is of great significance for the sustainable development and utilization of ecosystems. GDEs are defined as species, ecological communities, and their habitats that rely on groundwater to meet all or part of their water requirements(Rohde et al., 2024a). Groundwater provides GDEs with a stable water supply, regulates environmental temperatures, and offers unique chemical compositions, thus providing distinct habitat conditions for their biodiversity(Rohde et al., 2021). Based on the ecological value of groundwater, GDEs can be categorized into three types: (a) aquifer and cave ecosystems; (b) spring, wetland, river, estuary, and near-shore marine ecosystems; and (c) terrestrial vegetation ecosystems(Link et al., 2023). Identifying whether an ecosystem depends on groundwater is fundamental to GDEs research(Liu and Liang, 2020). GDEs not only exhibit high species richness and carbon sequestration capacity but also play significant roles in buffering stormwater runoff and purifying pollutants(Yang and Liu, 2020).

Currently, research on GDEs primarily focuses on their identification and mapping, risk assessment, the interaction between groundwater and surface vegetation, and management strategies(Martínez-Santos et al., 2021; Jeevarathinam et al., 2013; Rohde et al., 2019; Esteban and Dinar, 2016). Among the methods for GDEs identification, field-scale recognition is typically based on observational experiments and field surveys(Hoogland et al., 2010), while regional-scale identification generally relies on remote sensing technologies(Brim Box et al., 2022; Castellazzi et al., 2019). For example, research by Melissa M. Rohde et al. employed a random forest machine learning model to achieve global-scale identification(Rohde et al., 2024b). However, few studies have integrated field-measured data with remote sensing data for region- and site-scale GDEs identification. Regional-scale identification of GDEs often involves spatial analysis using tools such as remote sensing and Geographic Information Systems (GIS) (Xu et al., 2022b; Liu et al., 2021b), typically incorporating remote sensing-based indicators like the Normalized Difference Vegetation Index (NDVI), Enhanced Vegetation Index (EVI), Leaf Area Index (LAI), and humidity indices such as the Normalized Difference Water Index (NDWI) and the Topographic Wetness Index (TWI), combined with hydrological and meteorological data like water table depth (WTD), evapotranspiration (ET), Digital Elevation Models (DEM), and precipitation. However, these indicators often lack integration with field data, such as vegetation root depth and soil types (Torres-García et al., 2021; Zurek et al., 2015). To validate GDEs identification, correlation and regression analyses are commonly employed to assess the relationship between the results and actual data(Otoo et al., 2024; Xu et al., 2022a), or field validation methods(Gow et al.; Li et al., 2024; Brim Box et al., 2022) are used, which may limit the accuracy and reliability of the results.



65 This study presents a refined mapping approach for GDEs that integrates geospatial technologies with field-measured data. The methodology: (a) enables the periodic identification of GDEs in the Urumqi River Basin and Chai Wo-pu Lake Basin to examine their multi-year variation characteristics; (b) generates high-precision distribution maps of GDEs probability in typical regions through field investigations of vegetation root depth and water table depth; (c) compared to previous studies, this approach integrates remote sensing data with field-measured data to link GDEs identification at both regional and site
70 scales, thus eliminating the influence of factors such as human irrigation. This method provides valuable insights for the precise identification and assessment of GDEs in arid and semi-arid regions and can serve as a basis for the classification, zoning, management, and conservation of regional GDEs.

1 Materials and Methods

1.1 Study Area

75 The study area encompasses the Urumqi River and Chai Wo-pu Basin, located in the central part of the Xinjiang Uygur Autonomous Region, China, at the northern foothills of the Tianshan Mountains. The total area is 9,182 km² (Figure 1). The Urumqi River originates at the main peak of Mount Karauchen in the northern Tianshan range, at an elevation of 3,800 meters. It flows northward through the Urumqi urban area and eventually disappears at the southern edge of the Junggar Basin. The river is 214.3 km long and connects with the Banfanggou and Toutunhe river basins to the east and west,
80 respectively. The Chai Wo-pu Basin lies between two uplifted fault-block mountain ranges: the Bogda Mountains to the north and the Yilin Habirga Mountains to the south. The lowest point in the basin, located south of the Great Salt Lake, has an elevation of 1,072 m. The entire study area is situated in the interior of the Eurasian continent, surrounded by high mountains to the east, south, and west, with the terrain gradually descending to the north. The study area is distant from the ocean and experiences a temperate continental arid climate (Wang et al., 2024). The region exhibits significant temperature and precipitation variation, with an average annual temperature of 5.7°C and a summer-winter temperature difference of
85 38.9 °C (Song et al., 2019). Annual precipitation ranges from 70 to 500 mm, with higher precipitation in the mountainous areas compared to the plains and valleys. The northern desert region receives less than 100 mm of precipitation (Sun et al., 2015), and the multi-year average evapotranspiration ranges from 22.74 to 479.33 mm (Pandey et al., 2023).

The study area is an ecologically fragile region with significant groundwater development and severe water conflicts,
90 making it a sensitive area for global climate change impacts (Mamattursun et al., 2022b). Typical groundwater-dependent inland wetland and desert ecosystems are found in the lower reaches of the Urumqi River Basin (Dongdao Haizi) and along the lakeshore of Chai Wo-pu Lake. With increasing exploitation of local water and soil resources and the intensification of climate change, the region has experienced substantial changes in its water balance. The health of GDEs is deteriorating, and several regional ecological issues have emerged, including continuous declines (or localized rises) in groundwater levels,
95 shrinking wetland areas, salinization, and desertification (Zhang et al., 2021). To understand the evolution of GDEs in the



study area, this research conducted an identification and classification of GDEs based on their likelihood. The findings provide a basis for implementing classification, zoning, and protection strategies for local GDEs.

1.2 Data Collection and Processing

1.2.1 Precipitation and Evapotranspiration Data

100 One of the key methods for assessing plant dependence on groundwater is through water balance measurements or
calculations. When a plant's water utilization exceeds the availability of precipitation, soil water, and surface water from
rivers and wetlands, it indicates a reliance on groundwater. Therefore, the difference between evapotranspiration and
precipitation is considered an important indicator of the likelihood of GDEs in a region. Remote sensing technology has been
widely applied in water balance studies, particularly in evapotranspiration mapping. In arid and semi-arid regions, when
105 evapotranspiration exceeds precipitation, it suggests that terrestrial ecosystems, including vegetation, may primarily rely on
groundwater during dry periods to meet their water demands rather than on precipitation.

To minimize the potential impact of precipitation on vegetation ecosystems, this study first identified relatively dry years
prior to the identification of GDEs. Monthly precipitation data from the Urumqi station, sourced from the China
Meteorological Data Network (<http://data.cma.cn>), were used. Given data availability, the study selected the period from
110 1998 to 2020 for evaluation and calculated the annual precipitation for the Urumqi River and Chai Wo-pu Basins. Based on
years of low precipitation and consecutive droughts, and considering the principle of temporal proximity, the study selected
2001, 2006, 2014, 2020, and 2023 as the years for GDEs identification. Since vegetation water usage is typically higher in
the later stages of the growing season, and potential evapotranspiration is more intense during this time, August was chosen
for GDEs identification. Precipitation data were obtained from the China 1 km resolution monthly precipitation dataset (Peng,
115 2024a), which has a spatial resolution of 0.0083° (approximately 1 km) and a temporal resolution of 1 month. In ArcGIS, the
precipitation raster data were resampled to a 30 m resolution using the nearest neighbor method, and precipitation images for
the selected years in August were extracted using band extraction.

Due to the difficulty in acquiring actual evapotranspiration data, this study used potential evapotranspiration data, which
reflects the maximum evapotranspiration under ideal conditions. In arid and semi-arid regions, areas with higher potential
120 evapotranspiration typically correspond to shallow groundwater areas with vegetation growth. Higher potential
evapotranspiration values suggest that vegetation may be utilizing groundwater. Potential evapotranspiration data were
obtained from the China 1 km monthly potential evapotranspiration dataset (Peng, 2024b), with a spatial resolution of
 0.0083° (approximately 1 km) and a temporal resolution of 1 month. In ArcGIS, the potential evapotranspiration raster data
were resampled to a 30 m resolution using the nearest neighbor method, and potential evapotranspiration images for the
125 selected years in August were extracted using band extraction.



1.2.2 Land cover type and vegetation coverage data

Direct field surveys for GDEs identification are feasible at small scales but impractical for large areas, and they cannot capture temporal changes in regional environments (Vargas et al., 2019). Therefore, satellite-derived data have become a common tool for assessing ecological environments. In the past decade, the use of remote sensing data in GDEs identification and mapping has increased significantly (Xu et al., 2022b; Liu et al., 2021b; Eamus et al., 2015), with numerous continuously monitored satellites providing a wealth of spectral information that is freely available.

Fractional Vegetation Cover (FVC) is a crucial indicator of regional ecological environment quality, influenced by factors such as topography (elevation and slope), precipitation, temperature, soil characteristics, and population distribution (Wang et al., 2023; He et al., 2023; Yan et al., 2020). Therefore, understanding the long-term changes in regional FVC is essential for understanding the natural and anthropogenic factors affecting vegetation growth. Among remote sensing data, NDVI is highly correlated with vegetation biomass in ecosystems (He et al., 2023), making it an important tool for studying vegetation distribution and changes. NDVI data have been widely used to assess vegetation changes and are a key parameter in calculating FVC. Additionally, NDVI shows a good correlation with groundwater, making it a suitable indicator for shallow groundwater storage conditions (Huang et al., 2020).

The spectral data for this study were derived from Landsat-5 satellite imagery, with a spatial resolution of 30 meters. The Random Forest (RF) algorithm was used to classify land cover types, following the national land resource classification system. Land use was divided into six main categories: cropland, forestland, grassland, water bodies, built-up areas, and unused land. Based on these categories, secondary land classifications were added according to the classification system from the Institute of Geography, Chinese Academy of Sciences, resulting in a total of 17 subclasses. Using this approach, the distribution of cropland and built-up areas in the study area for 2023 was obtained, and the classification results were evaluated for accuracy using overall accuracy and the Kappa coefficient.

For each research period, images with cloud cover less than 10% during the months of June to September (the peak growing season) were selected to calculate NDVI values. The Maximum Value Composite (MVC) method was applied to calculate NDVI values during the peak vegetation cover period. Prior to calculation, the original remote sensing images underwent preprocessing, including radiometric calibration, layer stacking, atmospheric correction, and image fusion and clipping. A pixel binary model was employed to invert FVC and subsequently, drone imagery was calibrated and converted for use with machine learning algorithms to improve calculation accuracy. The FVC calculation formula is as follows:

$$FVC = \frac{NDVI - NDVI_{soil}}{NDVI_{veg} - NDVI_{soil}} \times 100\% \quad (1)$$

Where FVC represents the vegetation fraction cover (%); $NDVI$ is the calculated Normalized Difference Vegetation Index, which is dimensionless; $NDVI_{soil}$ is the value for pixels with bare soil or no vegetation cover, which can be determined by the low percentile of the regional pixel distribution, such as the 5th percentile; $NDVI_{veg}$ is the $NDVI$ value for fully vegetated pixels, which is determined based on the actual conditions of the study area, typically by the high percentile of the regional pixel distribution, such as the 95th percentile.



1.2.3 Terrain Wetness Index (TWI) Data

160 Topography significantly influences groundwater depth, which, in turn, affects the distribution of GDEs. The elevation of the terrain directly influences the spatial distribution of groundwater levels and hydrological processes, creating distinct water accumulation and drainage zones that lead to uneven water distribution. The nature of the surface terrain causes moisture accumulation, which results in groundwater infiltration and recharge (Pandey et al., 2023). The TWI is a physical indicator used to measure the impact of regional topography on runoff direction and accumulation. Areas with higher TWI values are typically found in lower parts of the landscape and are closely associated with groundwater. TWI is calculated based on local DEM data, which in this study was sourced from the global ASTER GDEM released by NASA in 2011, with a spatial resolution of 30 meters. The formula for calculating TWI is as follows:

$$TWI = \ln \left(\frac{CA}{Slope} \right) \quad (2)$$

Where *CA* represents the local upslope contributing area drained through each grid cell, and *Slope* is the steepest outward slope for each grid cell, measured as the elevation difference over distance, i.e., the tangent of the slope angle, which indicates long-term soil moisture availability. *TWI* was calculated using ArcGIS 10.8.

1.2.4 Root Depth and Groundwater Depth Data

Field surveys provide essential ground-truth data to verify the accuracy of remote sensing data and its interpretation, making them an indispensable part of the GDEs identification process. Root depth and groundwater depth are critical parameters for GDEs investigation and identification (Martínez-Santos et al., 2021; Xu et al., 2022b; Liu et al., 2021b). By analyzing the relationship between vegetation root systems and groundwater levels, it is possible to determine whether an area is a GDE. If the vegetation roots can reach the groundwater table, it indicates that the plants can directly absorb groundwater to meet their growth needs, thereby classifying the ecosystem as a GDE (Merz, 2011).

Based on the regional vegetation distribution obtained through remote sensing interpretation, this study employed ecological probing methods to investigate root systems in sample areas with finer roots, such as herbaceous plants. Using the locations of vegetation sample plots in the region, ecological shallow drilling points were determined. A total of 43 points were established in typical areas (Figure S1 in the Supplement provides detailed information on the coordinate distribution) to collect root depth data for the vegetation in the region.

Guided by the groundwater level distribution pattern, and in alignment with the needs of the GDEs investigation, existing well and spring resources were fully utilized to measure groundwater depth. In accordance with the "Hydrogeological Survey Specifications (1:50000)" (DZ/T0282-2015), 100 monitoring points were established in typical areas (Figure S2 in the Supplement provides detailed information on the coordinate distribution) to collect groundwater depth data for the region. These data are crucial for assessing the likelihood of GDEs and provide scientific support for further ecological protection and water resource management.



190 1.3 Methods

1.3.1 GDEs Identification and Likelihood Evaluation Process

The identification of Groundwater Dependent Ecosystems (GDEs) primarily involves two key components (Figure 2): identifying potential areas and accurately identifying typical areas. The process is divided into five steps: (a) Determine the Research Year and Study Area; (b) Assess Groundwater Use in the Study Area Using Remote Sensing, Meteorological, 195 Topographic, and Field Data; (c) Standard Layer Analysis and Classification; (d) Map the GDEs Identification Results; (e) Verification and Application of the Identification Results.

1.3.2 Delineation of Potential Areas and Typical Areas

The focus of GDEs identification lies in natural vegetation areas. In this study, the first step is to exclude hydrogeological types that are not closely related to groundwater and land use types that are significantly influenced by human activities. In 200 arid inland river basins, vegetation in upstream mountainous areas primarily depends on surface water or snowmelt. For instance, in the upstream mountainous areas of the Urumqi River Basin, vegetation such as herbaceous plants and mid-to-low mountain forests rely mainly on precipitation and snowmelt in the mountains (Chen et al., 2014). Based on the hydrogeological zoning from the "Comprehensive Evaluation Report on Water Resources of the Urumqi River Basin, Xinjiang Uygur Autonomous Region" (Xinjiang Geological and Mineral Bureau, First Hydrogeological and Engineering 205 Geological Team, 1985), pixels representing bedrock mountainous areas are excluded. And following the principle of using the most recent data, land use data for 2023 is utilized. After excluding cultivated land and construction land types, the natural vegetation areas mainly include wetlands, forests, grasslands, and unused land. The land use data used in this study is derived from Landsat satellite imagery for June to September 2023 (<https://earthexplorer.usgs.gov>), with a spatial resolution of 30 meters and a temporal resolution of 16 days. The dataset consists of six main categories: cultivated land, forests, 210 grasslands, water bodies, construction land, and unused land. Finally, areas with a high association with groundwater are extracted as potential areas for GDEs identification.

To refine the identification of GDEs and achieve high-accuracy likelihood classifications, additional data are collected through field surveys. Based on the identified GDEs areas, regions within the study areas that exhibit high vegetation quality, rich species diversity, and significant groundwater exposure are selected as typical areas for further identification. These 215 areas are often critical for maintaining local ecological balance. Analyzing the GDEs likelihood in these regions can provide valuable insights for the refined management and protection of GDEs.

1.3.3 GDEs Identification

The K-means algorithm (Hartigan and Wong, 1979) was selected to classify each standard image. This unsupervised classification method can automatically detect similar clusters without requiring prior knowledge, making it suitable for 220 identifying potential areas in the absence of previous studies. FVC, ET-P, and WTI were used as the classification criteria to



group each pixel within the potential area into five clusters, with $k=5$ as the classification parameter. A higher cluster value indicates a greater dependence of vegetation on groundwater. The values for each pixel, based on the assigned standards, were summed, resulting in a range from 3 to 15. The final classification was divided into five categories representing the likelihood of GDEs existence: very likely (12 to 15), likely (10 to 11), neutral (8 to 9), unlikely (6 to 7), and very unlikely (3 to 5) (Liu et al., 2021a). The processing was carried out using ENVI 5.3 (Exelis VIS) and ArcGIS 10.2.

1.3.4 GDEs Identification Result Validation

1.3.4.1 Wetland Ecosystem Validation

Previous studies have shown that wetland ecosystems in arid regions are typically groundwater-dependent ecosystems (Hou, 2020; Münch and Conrad, 2007). The GDEs identification results were validated by comparing them with the locations of marsh wetlands. Wetland data for validation were sourced from GWL_FCS30: The 2020 Global 30 m Wetland Map and Fine Classification System, which has a spatial resolution of 30 m. The validation was conducted using the "Producer's Accuracy" method, which calculates the percentage of overlap between the result data and reference data. This method is widely used for accuracy evaluation (Congalton, 1991). The calculation yields the ratio of the overlap area between the two datasets to the reference area, as shown in the following formula:

$$PA = \frac{AREA_{overlap}}{AREA_{reference}} \quad (3)$$

Where $AREA_{overlap}$ is the overlapping area of the calculated data (km^2); $AREA_{reference}$ is the area of the reference data (km^2).

1.3.4.2 Field Validation

A random sample of 100 points, categorized as "very likely" or "likely" GDEs, was selected for field validation. On-site investigations were conducted using GPS, and the geographical coordinates of each point were transferred to GIS for further processing.

1.3.4 GDEs Identification Result Validation

To determine whether plant roots can access groundwater resources, three datasets—related to hydrogeology (groundwater depth), soil texture and vegetation (rooting depth)—were integrated. To assess actual groundwater usage by plant roots, the root depth and capillary rise height were summed to estimate the maximum depth of water absorption. This value was then compared with the groundwater depth. If the plant's groundwater utilization depth exceeds the groundwater depth, plants are considered to rely on groundwater. The difference between the plant's groundwater utilization depth and the groundwater depth is referred to as the Vegetation Groundwater Utilization Index (VGUI). The formula for calculating VGUI is as follows:

$$VGUI = (H_{root} + H_c) - WTD \quad (4)$$

In the formula, WTD refers to the water table depth (m); H_{root} is the root depth obtained through interpolation based on field survey data (m), and H_c is the capillary rise height corresponding to the soil. The capillary rise characteristics of the soil are



influenced by soil type. The effect of vadose zone lithology and structure on plants can be indirectly reflected by the capillary rise characteristics of the soil. The empirical values of capillary water rise for different soil types are obtained from Table 1, as shown below.

255 In the identification of GDEs in typical areas, the K-means algorithm was applied to classify four images: FVC, ET-P, WTI, and VGUI. The values for each pixel, derived from the summed results, range from 4 to 20. The final output is categorized into five groups, representing the likelihood of GDEs existence: Very Likely (17 to 20), Likely (14 to 16), Neutral (11 to 13), Unlikely (8 to 10), and Very Unlikely (4 to 7). The data processing was performed using ENVI 5.6 and ArcGIS 10.8 software.

260 **2 Results and Analysis**

2.1 Potential Area Identification Results

2.1.1 Determination of Potential Area

Based on existing research, this study initially delineated areas with a higher correlation to groundwater, focusing on the exclusion of non-GDE areas and identifying the remaining areas as potential GDEs. As shown in Figure 3a, the potential areas in the Urumqi River and Chai Wo-pu Basin are primarily located in the Chai Wo-pu Basin, the mouth of the Urumqi River, the Dabancheng region and areas to the north, the lower reaches of the Urumqi River, and the Dongdao Haizi area. The total area of these potential GDEs is 4,197.89 km², accounting for 44.8% of the total area of the Urumqi River and Chai Wo-pu Basin.

2.1.2 Standard Layer Mapping Results

270 In this study, remote sensing images, evapotranspiration, precipitation, and digital elevation data from the Urumqi River and Chai Wo-pu Basin for the years 2001, 2006, 2014, 2020, and 2023 were used to derive three standard layers related to vegetation greenness (FVC), meteorological conditions (evapotranspiration and precipitation difference), and terrain (TWI). Based on the FVC mapping results (Figure S3), areas with higher vegetation cover were predominantly located around water bodies and groundwater discharge zones. In contrast, areas with lower vegetation cover were primarily found in the Gobi desert of the Chai Wo-pu Basin, grasslands with sparse coverage, and the southern edge of the Junggar Desert downstream of the Urumqi River. Inter-annual variations in FVC revealed significant changes in regions such as Baiyanggou in the upper reaches of the Urumqi River, the foothill valleys south of Aksu, and the northern edge of the Junggar Desert, excluding the Urumqi urban area. This phenomenon is likely attributed to the unique geographical environment of the Urumqi River and Chai Wo-pu Basin, characterized by a combination of high mountains and deserts in an arid region, where temperature and precipitation have a substantial impact on the basin.

280



Based on the mapping results of ET-P (Figure S4), the ET-P values in the downstream areas of the Urumqi River are significantly higher than those in the upstream regions, and the ET-P values in the plains of the Chai Wo-pu Basin are also notably higher than those in the surrounding mountainous areas. High ET-P areas are primarily located in the downstream region of the Urumqi River, extending from the northern part of Urumqi City to the southern edge of the Junggar Desert, as well as across the Chai Wo-pu Basin. These areas receive very little annual precipitation and are predominantly covered by desert and barren land, subject to prolonged direct sunlight. By comparing interannual variations in ET-P, noticeable potential changes in groundwater use are observed in the Dongdao Haizi region of the downstream Urumqi River and at the exit of the Urumqi River in the upstream region. The Dongdao Haizi region lies at the boundary between oasis and desert, where evapotranspiration shows considerable variation across different years, particularly in August. In contrast, the Urumqi River exit area, which has a relatively high elevation, experiences significant interannual variation in evapotranspiration during August, largely due to fluctuations in precipitation.

According to the TWI mapping results (Figure S5), areas with high TWI are consistent with areas of high water content, primarily located around Chai Wo-pu Lake, the Great Salt Lake, the Small Salt Lake, and parts of the area south of Dongdao Haizi to the north. Low TWI areas are mainly found in the southern and eastern mountainous regions, which aligns closely with the hydrological and geological zoning results of the region.

2.1.3 GDEs Potential Area Identification Results

The GDEs identification results are depicted in Figure 4, the study area is classified into five categories: Very Likely, Likely, Neutral, Unlikely, and Very Unlikely, which represent varying degrees of groundwater dependence of ecosystems. A comprehensive analysis of data from the five years reveals that the areas most likely to be GDEs are predominantly located in groundwater discharge zones, such as Dongdao Haizi, Chai Wo-pu Lake, Salt Lake, and surrounding regions, where significant interaction between surface water and groundwater occurs in flat areas. The areas with a likely GDEs status are spatially similar to the very likely GDEs areas but cover a larger extent, spanning from the northern part of the Urumqi River downstream to the southern edge of the Junggar Desert. These areas are characterized by flat terrain and a higher degree of aridity. Regions with a moderate likelihood of being GDEs include small valleys in higher regions, parts of the northern desert plains, and the central plains of the Chai Wo-pu Basin. Areas classified as unlikely or very unlikely to be GDEs account for only 16.6% of the surveyed area.

By comparing the interannual variations in GDEs likelihood, as shown in Figure 4f, regions with different GDEs likelihood levels exhibit irregular fluctuations over time. Between 2006 and 2023, areas identified as "unlikely" or "very unlikely" for GDEs showed a gradual increase, with the expansion concentrated in the upper reaches of the Urumqi River and the higher parts of the watershed. The area grew from 370.2 km² in 2006 to 785.5 km² in 2023, representing a growth rate of 112.2%. Regions with moderate and likely GDEs potential remained relatively stable, with dynamic changes observed in the northern Urumqi River downstream desert areas and the southern margin of the Junggar Desert. These areas, characterized by low surface cover and significant surface evapotranspiration, are more sensitive to temperature and precipitation variations. The



315 area of regions deemed "very likely" for GDEs showed a slight, steady increase from 364.75 km² in 2001 to 498.03 km² in
2023, with a growth rate of 36.5%. These areas are primarily located in the groundwater discharge zone around Dongdao
Haizi in the lower reaches of the Urumqi River. This trend aligns with the increased focus on water resources and the
ecological environment in the area since 2000. Several key reports have been developed, including the "Dongdao Haizi
Shoreline Protection and Utilization Planning Report" and the "Urumqi City Midong District Dongdao Haizi Management
Area Delimitation Report." Furthermore, ecological management objectives for the area have been incorporated into the
320 "14th Five-Year Plan for Ecological and Environmental Protection in Urumqi."

2.2 Validation Results

2.2.1 Wetland Ecosystem Validation

325 Based on the locations of areas identified as "very likely" and "likely" GDEs, the validation scope was determined, and the
subset validation areas were delineated by combining the spatial distribution of marsh wetlands, as shown in Figure 5. Using
the "Producer's Accuracy" method, the overall validation accuracy of the GDEs identification results was 84.1%. For the
subset validation areas, Figure 6a shows the Dongdao Haizi wetland area (4.12 km²), with a validation accuracy of 95.6%;
Figure 6b shows the lake and reservoir area (7.37 km²), with a validation accuracy of 69.8%; and Figure 6c shows the Chai
Wo-pu Lake wetland area (8.17 km²), with a validation accuracy of 91.2%. These results indicate that the GDEs
330 identification method based on remote sensing data can effectively identify areas with high groundwater dependency, such
as local lakes and reservoirs, with relatively high accuracy.

2.2.2 Wetland Ecosystem Validation

335 Based on field survey results, 100 sampling points were selected from areas identified as "very likely" and "likely" GDEs for
validation, and all of these points were confirmed as GDEs. During the field investigation, the presence of plants in
groundwater discharge zones, as well as deep-rooted trees and shrubs along natural moisture gradients, indicated GDE
locations. At 14 of the field survey points, a decline in vegetation health and vitality was observed, reflecting the ecological-
hydrological response of these ecosystems to hydrological and climatic changes, as well as anthropogenic impacts since
2001. Observations were made of both terrestrial and aquatic GDEs (mainly terrestrial), including grasslands, shrubs, springs,
forests, riparian vegetation, and estuarine wetlands. Photographs taken at 20 selected validation points are shown in Figure 6.

2.3 GDEs Typical Area Field Precision Identification Results

340 2.3.1 Determination of Typical Areas

Based on the results of potential GDEs identification, areas with a higher likelihood of GDEs, characterized by good
vegetation coverage, species richness, and extensive groundwater discharge zones, were selected for further investigation.
The focus was placed on the Dongdao Haizi and desert-oasis transition zone, as well as the areas surrounding Chai Wo-pu



Lake and the large and small salt lakes. Two typical areas, each covering 500 square kilometers, were delineated for on-site
345 field investigation and precise GDEs identification (Figure 7).

2.3.2 Spatiotemporal Changes and Mapping of Vegetation Groundwater Uptake Index

The study collected data on vegetation root depth and groundwater depth in the typical areas in 2023 through field surveys. By integrating
these data with the capillary rise heights corresponding to the soil type, a standard layer (Layer 4) representing the vegetation's
groundwater uptake index was developed. The distribution of vegetation root systems, soil types, groundwater depth, and the resulting
350 VGUI for the northern and southern typical areas are shown in Figure S6.

In the northern typical area, the distribution of the vegetation groundwater uptake index is closely aligned with groundwater
depth, exhibiting distinct spatial patterns. From south to north, and from the upper to the lower reaches of the Urumqi River,
the vegetation groundwater uptake index gradually increases, reaching its highest value in the northernmost region along the
Dongdao Haizi groundwater discharge zone. This trend suggests that vegetation in this area progressively relies more on
355 groundwater resources. In the southern typical area, the vegetation groundwater uptake index is generally lower than in the
northern area, with higher values observed around Chai Wo-pu Lake and the salt lakes, which correlate with groundwater
depth distribution.

2.3.3 Precise Identification of GDEs in Typical Areas

The GDEs identification results of typical areas are depicted in Figure 8, the typical areas were classified into five
360 categories: very likely, likely, moderate, unlikely, and very unlikely. The spatial distribution of GDEs likelihood largely
aligns with the results of the potential area identification. In the northern typical area, regions classified as "very likely" and
"likely" GDEs are primarily concentrated in the northern part, including the Dongdao Haizi area and its surroundings, as
well as some agricultural irrigation areas between Mengjin Reservoir and Bayi Reservoir. These findings are consistent with
the field survey results. The "unlikely" GDEs regions are mainly located in the southern part of the typical area,
365 corresponding to areas of construction land. These areas exhibit low vegetation coverage, significant anthropogenic impact
on surface vegetation, and weak groundwater association. Compared to the northern typical area, the southern typical area
has a lower overall likelihood of GDEs. The "very likely" and "likely" GDEs regions in the southern area are primarily
concentrated around Chai Wo-pu Lake, the salt lakes, and the groundwater discharge zones in the southeastern part, which is
consistent with the field survey findings. The "unlikely" GDEs regions are predominantly found in the mountainous areas at
370 the northern and southern edges of the Chai Wo-pu Basin, as well as in the northwestern industrial zones. These areas are
characterized by deep groundwater levels and are more affected by climate change. Industrial zones, which are typically
hardened, alter the natural vegetation growth environment, leading to significant anthropogenic degradation of the ecological
environment.

By comparing the GDEs identification results before and after incorporating the vegetation groundwater uptake index
375 (standard layer 4) and using ArcGIS Pro 3.3.1 for change detection, it was found that the inclusion of standard layer 4



reduced the likelihood of GDEs in 41.0% of the typical areas. These regions are mainly concentrated in cultivated and construction lands, which account for 64.9% of the areas where the likelihood decreased. Over 50% of this reduction occurred in agricultural areas, indicating that the inclusion of standard layer 4 helps eliminate the interference from human irrigation and other factors in GDEs identification.

380 **3 Discussion**

This study integrated remote sensing, hydrological, meteorological, and field survey data to evaluate the likelihood of GDEs using multiple indicators, including FVC, ET-P, WTI and VGUI. These indices collectively reflect the region's dependence on groundwater. The VGUI, a new quantitative index, combines several field survey parameters, such as groundwater depth, soil type and vegetation root depth, providing a more direct and accurate measure of vegetation's
385 groundwater uptake. During the mapping of each index, the K-means algorithm was used to classify the standard layers, facilitating the identification of potential GDEs regions in areas lacking prior GDEs data. This multi-stage approach, encompassing both potential area identification and typical area verification, enhanced the precision and reliability of GDEs recognition.

The study found that the likelihood of GDEs is higher in the downstream regions of the Urumqi River, particularly
390 around Dongdao Haizi, Chai Wo-pu Lake, and the salt lakes. These areas feature relatively shallow groundwater depths, and the strong to moderate correlation between WTD and NDVI clusters aligns with findings from other studies, which suggest that shallower groundwater increases the likelihood of GDEs occurrence (Eamus and Froend, 2006). Since 2000, the average FVC in the Urumqi River Basin has shown a slow upward trend, ranging from -10% to +10% (Mamattursun et al., 2022a) [4]. This trend is consistent with Liu et al.'s analysis of the entire Xinjiang region,
395 where the likelihood of GDEs in desert areas decreased, while in oasis areas, it increased significantly (Liu et al., 2018). This shift can be partly attributed to long-term vegetation restoration efforts aimed at combating desertification. Increased vegetation cover has improved soil water retention and infiltration capacity; however, the ET of ecological restoration plants is significantly higher than that of natural vegetation, leading to excessive soil moisture depletion and further reduction in groundwater storage, thus disrupting the water balance (Xu et al., 2022a). These findings
400 highlight significant spatial variation in GDEs likelihood. Theoretically, because vegetation roots generally cannot access deep groundwater directly, vegetation is unlikely to be part of GDEs in areas where WTD exceeds 20 m (Liu et al., 2021a). However, some studies suggest that the groundwater depth threshold for GDEs could be around 20 m (Páscoa et al., 2020). Based on field data collected in 2023, groundwater depths in the southern region of Chai Wo-pu Lake and along the Tianshan foothills range from 30 to 60 m, with groundwater depth being positively correlated with
405 topography. In contrast, areas influenced by surface water from rivers in the eastern part of the basin have relatively shallow groundwater depths (10-30 m). GDEs with moderate or higher groundwater dependence were identified in the

southwestern and eastern parts of the Chai Wo-pu Basin. This finding is consistent with other studies, which suggest that in arid regions, plant roots can reach groundwater depths of 20 m or more. For example, in the Karez wells of Turpan, roots of *Alhagi* species have been found below 20 m. In dry regions, plants such as *Populus euphratica*,
410 *Zygophyllum* spp., and *Tamarix* spp. have deep roots, some of which extend more than 10 m, allowing them to access deeper groundwater either directly or through capillary rise (Xinjiang Institute of Ecology and Geography, 2010).

Although this study provides valuable insights into the identification and mapping of GDEs, it has several limitations. The drought period is often referenced in GDEs identification and mapping methods (Páscoa et al., 2020; Liu et al., 2021a), but the classification of drought severity lacks consistency. This study, for example, only considers the most
415 recent year in which precipitation consistently declined. The absence of sufficient groundwater monitoring data and limitations in spatial visualization accuracy also impacted the validation results. Additionally, while the study integrated soil type to estimate capillary rise heights for evaluating vegetation's potential to use groundwater, the impact mechanism of capillary rise is complex and influenced by factors such as soil particle size distribution, soil structure, bulk density, mineral composition, moisture content, temperature, and porosity. Further research is required
420 to better understand these dynamics. Furthermore, arid and semi-arid regions are particularly vulnerable to both natural and anthropogenic influences (Amantai and Ding, 2021), which may have affected the findings. The study focused on groundwater-dependent ecosystems in these regions, but future work could explore the effects of human interventions, such as land reclamation, irrigation, and industrial activities, which are especially pronounced in semi-arid areas.

Despite these limitations, the study successfully identified potential GDEs and analyzed their multi-year
425 variations, incorporating field data for precise identification. This approach allows for the identification of GDEs across different likelihood levels in typical regions. Overall, the methodology developed in this study is applicable to other arid and semi-arid regions, providing an effective framework for accurately identifying and monitoring GDEs.

4 Conclusion

This study introduces a new geospatial method that integrates remote sensing, meteorological, hydrological, and field survey
430 data to effectively map GDEs and analyze their spatiotemporal variations. The K-means algorithm was applied to classify four standard layers, including FVC, ET-P, WTI and VGUI. Among these, FVC, ET-P and WTI were used to identify potential areas, with GDEs maps from 2001, 2006, 2014, 2020, and 2023 revealing regions with varying likelihoods of being GDEs (very likely, likely, moderately likely, unlikely, and very unlikely). Wetland ecosystem comparisons showed a validation accuracy of 84.1% for the potential GDEs identification results. Field surveys confirmed that 100% of the
435 surveyed points corresponded to GDEs. The identification results show that the groundwater overflow zones of Dongdaohaizi, Chaiwopu Lake, Salt Lake and surrounding areas are the areas with the highest probability of GDEs (very likely and likely), and the area of non-GDE (very unlikely and unlikely) has increased significantly in recent years. By



incorporating the VGUI, a field-survey-based standard layer, precise GDEs identification for 2023 was achieved. Compared to the results from the three other standard layers, the inclusion of VGUI further reduced interference from factors such as human irrigation in GDEs recognition.

This study conducted GDEs identification at different scales, focusing on the temporal changes in GDEs likelihood within potential areas, while also increasing field survey data for precise identification in typical regions. This approach provides a scientific reference for local environmental management agencies in monitoring ecological changes and formulating management strategies. The methodology is applicable to other arid and semi-arid environments, contributing to the sustainable management of GDEs amid ongoing climate and anthropogenic changes.

Data availability

The data that support the findings of this study are available from the corresponding author upon reasonable request.

Author contributions

All authors contributed to the study conception and design. Zhihao Ye, Rui Meng and Qiang Zhou designed the research project and contributed to data analysis and interpretation. Mingxia Zheng, Xiaoyu Zhang and Longhao Huang help analyzed the data. Liansheng He prepared materials. Xin Zhou and Liansheng He are the corresponding author.

Competing interests

The contact author has declared that none of the authors has any competing interests.

Acknowledgements

We thank the Institute of Water Ecology, Chinese Academy of Environmental Sciences and the State Key Laboratory of Environmental Benchmarking and Risk Assessment, Chinese Academy of Environmental Sciences for providing technical support and experimental sites for this study. Thanks to the College of River and Ocean Engineering of Chongqing Jiaotong University and Beijing Zhongdi Hongke Environmental Technology Co., Ltd. for their help in the on-site investigation.

Financial support

This research was supported by National key research and development program, Technical system and countermeasures of priority control of pollutants in manufacturing enterprises (No.2022YFC3703104).



References

- Amantai, N. and Ding, J.: Analysis on the Spatio-Temporal Changes of LST and Its Influencing Factors Based on VIC Model in the Arid Region from 1960 to 2017: An Example of the Ebinur Lake Watershed, Xinjiang, China, *Remote Sensing*, 13, 4867, 2021.
- Brim Box, J., Leiper, I., Nano, C., Stokeld, D., Jobson, P., Tomlinson, A., Cobban, D., Bond, T., Randall, D., and Box, P.: Mapping terrestrial groundwater-dependent ecosystems in arid Australia using Landsat-8 time-series data and singular value decomposition, *Remote Sensing in Ecology and Conservation*, 8, 464-476, <https://doi.org/10.1002/rse2.254>, 2022.
- Castellazzi, P., Doody, T., and Peeters, L.: Towards monitoring groundwater-dependent ecosystems using synthetic aperture radar imagery, *Hydrological Processes*, 33, 3239-3250, <https://doi.org/10.1002/hyp.13570>, 2019.
- Chen, W. T., Sun, Z. Y., Li, X. J., and Yang, J. C.: Remote sensing mapping of natural plant communities in arid inland areas: A case study of Dunhuang Basin, *Arid region geography*, 37, 1257-1263, 10.13826/j.cnki.cn65-1103/x.2014.06.020, 2014.
- Congalton, R. G.: A review of assessing the accuracy of classifications of remotely sensed data, *Remote Sensing of Environment*, 37, 35-46, [https://doi.org/10.1016/0034-4257\(91\)90048-B](https://doi.org/10.1016/0034-4257(91)90048-B), 1991.
- Duran-Llacer, I., Arumí, J. L., Arriagada, L., Aguayo, M., Rojas, O., González-Rodríguez, L., Rodríguez-López, L., Martínez-Retureta, R., Oyarzún, R., and Singh, S. K.: A new method to map groundwater-dependent ecosystem zones in semi-arid environments: A case study in Chile, *Science of the Total Environment*, 816, 14, 10.1016/j.scitotenv.2021.151528, 2022.
- Eamus, D. and Froend, R.: Groundwater-dependent ecosystems: The where, what and why of GDEs, *Australian Journal of Botany*, 10.1071/BT06029, 2006.
- Eamus, D., Froend, R., Loomes, R., Hose, G., and Murray, B.: A functional methodology for determining the groundwater regime needed to maintain the health of groundwater-dependent vegetation, *Australian Journal of Botany*, 54, 2006.
- Eamus, D., Zolfaghar, S., Villalobos-Vega, R., Cleverly, J., and Huete, A.: Groundwater-dependent ecosystems: recent insights from satellite and field-based studies, *Hydrology and Earth System Sciences*, 19, 4229-4256, 10.5194/hess-19-4229-2015, 2015.
- Esteban, E. and Dinar, A.: THE ROLE OF GROUNDWATER-DEPENDENT ECOSYSTEMS IN GROUNDWATER MANAGEMENT, *Natural Resource Modeling*, 29, 98-129, 10.1111/nrm.12082, 2016.
- Gibso, V. L., Bremer, L., Burnett, K. M., Lui, N. K., and Smith, C. M.: Biocultural values of groundwater dependent ecosystems in Kona, Hawai'i, *Ecology and Society*, 27, 10.5751/es-13432-270318, 2022.
- Gow, L., Brodie, R., Green, R., Punthakey, J., Woolley, D., Redpath, P., Bradburn, A., and Ltd, E.: Identification and monitoring GDEs using MODIS time series: Hat Head National Park – a case study,
- Hartigan, J. A. and Wong, M. A.: Algorithm AS 136: A K-Means Clustering Algorithm, *Journal of the Royal Statistical Society. Series C (Applied Statistics)*, 28, 100-108, 10.2307/2346830, 1979.
- He, X., Zhang, F., Cai, Y. F., Tan, M. L., and Chan, N. W.: Spatio-temporal changes in fractional vegetation cover and the driving forces during 2001-2020 in the northern slopes of the Tianshan Mountains, China, *Environmental Science and Pollution Research*, 30, 75511-75531, 10.1007/s11356-023-27702-x, 2023.
- Hoogland, T., Heuvelink, G. B. M., and Knotters, M.: Mapping Water-Table Depths Over Time to Assess Desiccation of Groundwater-Dependent Ecosystems in the Netherlands, *Wetlands*, 30, 137-147, 10.1007/s13157-009-0011-4, 2010.
- Hou, J. X.: Study on dynamics of shallow groundwater level and its relationship with vegetation in Yellow River Delta, 硕士, 10.27216/d.cnki.gysfc.2020.000090, 2020.



- Howard, J. K., Dooley, K., Brauman, K. A., Klausmeyer, K. R., and Rohde, M. M.: Ecosystem services produced by groundwater dependent ecosystems: a framework and case study in California, *Frontiers in Water*, 5, 2023.
- 505 Huang, F., Zhang, Y. D., Zhang, D. R., and Chen, X.: Environmental Groundwater Depth for Groundwater-Dependent Terrestrial Ecosystems in Arid/Semiarid Regions: A Review, *International Journal of Environmental Research and Public Health*, 16, 10.3390/ijerph16050763, 2019.
- Huang, F., Chunyu, X. Z., Zhang, D. R., Chen, X., and Ochoa, C. G.: A framework to assess the impact of ecological water conveyance on groundwater-dependent terrestrial ecosystems in arid inland river basins, *Science of the Total Environment*, 709, 10.1016/j.scitotenv.2019.136155, 2020.
- 510 Jeevarathinam, C., Rajasekar, S., and Sanjuán, M. A. F.: Vibrational resonance in groundwater-dependent plant ecosystems, *Ecological Complexity*, 15, 33-42, 10.1016/j.ecocom.2013.02.003, 2013.
- Li, M., Li, F., Fu, S., Chen, H., Wang, K., Chen, X., and Huang, J.: Identification, mapping, and eco-hydrological signal analysis for groundwater-dependent ecosystems (GDEs) in Langxi River basin, north China, *Hydrol. Earth Syst. Sci.*, 28, 4623-4642, 10.5194/hess-28-4623-2024, 2024.
- 515 Li, X., Chang, S. X., and Salifu, K. F.: Soil texture and layering effects on water and salt dynamics in the presence of a water table: a review, *Environmental Reviews*, 22, 41-50, 10.1139/er-2013-0035, 2014.
- Link, A., El-Hokayem, L., Usman, M., Conrad, C., Reinecke, R., Berger, M., Wada, Y., Coroama, V., and Finkbeiner, M.: Groundwater-dependent ecosystems at risk - global hotspot analysis and implications, *Environmental Research Letters*, 18, 10.1088/1748-9326/acea97, 2023.
- 520 Liu, C., Liu, H., Yu, Y., Zhao, W., Zhang, Z., Guo, L., and Yetemen, O.: Mapping groundwater-dependent ecosystems in arid Central Asia: Implications for controlling regional land degradation, *Science of The Total Environment*, 797, 149027, <https://doi.org/10.1016/j.scitotenv.2021.149027>, 2021a.
- Liu, C., Liu, H., Yu, Y., Zhao, W. Z., Zhang, Z., Guo, L., and Yetemen, O.: Mapping groundwater-dependent ecosystems in arid Central Asia: Implications for controlling regional land degradation, *Science of the Total Environment*, 797, 10.1016/j.scitotenv.2021.149027, 2021b.
- 525 Liu, Q. and Liang, Q. L.: Review of ecohydrological studies in groundwater dependent ecosystems, *Journal of Beijing Normal University: Natural Science Edition*, 56, 7, 2020.
- Liu, Y., Li, L., Chen, X., Zhang, R., and Yang, J.: Temporal-spatial variations and influencing factors of vegetation cover in Xinjiang from 1982 to 2013 based on GIMMS-NDVI3g, *Global and Planetary Change*, 169, 145-155, <https://doi.org/10.1016/j.gloplacha.2018.06.005>, 2018.
- 530 Mamattursun, A., Yang, H., Ablikim, K., and Obulhasan, N.: Spatiotemporal Evolution and Driving Forces of Vegetation Cover in the Urumqi River Basin, *International Journal of Environmental Research and Public Health*, 19, 15323, 2022a.
- Mamattursun, A., Yang, H., Ablikim, K., and Obulhasan, N.: Spatiotemporal Evolution and Driving Forces of Vegetation Cover in the Urumqi River Basin, *International Journal of Environmental Research and Public Health*, 19, 10.3390/ijerph192215323, 2022b.
- 535 Martínez-Santos, P., Díaz-Alcaide, S., De la Hera-Portillo, A., and Gómez-Escalonilla, V.: Mapping groundwater-dependent ecosystems by means of multi-layer supervised classification, *Journal of Hydrology*, 603, 10.1016/j.jhydrol.2021.126873, 2021.
- 540 Merz, S. K.: Australian groundwater-dependent ecosystems toolbox part 1: assessment framework, 2011.
- Münch, Z. and Conrad, J.: Remote sensing and GIS based determination of groundwater dependent ecosystems in the Western Cape, South Africa, *Hydrogeology Journal*, 15, 19-28, 10.1007/s10040-006-0125-1, 2007.



- Otoo, N. G., Sutanudjaja, E. H., van Vliet, M. T. H., Schipper, A. M., and Bierkens, M. F. P.: Mapping groundwater dependent ecosystems using a high-resolution global groundwater model, *Hydrol. Earth Syst. Sci. Discuss.*, 2024, 1-20, 545 10.5194/hess-2024-112, 2024.
- Pandey, H. K., Kumar Singh, V., Kumar Singh, S., and Kumar Sharma, S.: Mapping and validation of groundwater dependent ecosystems (GDEs) in a drought-affected part of Bundelkhand region, India, *Groundwater for Sustainable Development*, 23, 100979, <https://doi.org/10.1016/j.gsd.2023.100979>, 2023.
- Páscoa, P., Gouveia, C. M., and Kurz-Besson, C.: A Simple Method to Identify Potential Groundwater-Dependent Vegetation Using NDVI MODIS, *Forests*, 11, 147, 2020.
- Peng, S. Z.: 1km resolution Monthly Precipitation Dataset in China (1901-2023), National Tibetan Plateau Scientific Data Center [dataset], 10.5281/zenodo.3114194, 2024a.
- Peng, S. Z.: 1km Monthly Potential Evapotranspiration Data set in China (1901-2023), National Tibetan Plateau Scientific Data Center [dataset], 10.11866/db.loess.2021.001, 2024b.
- 555 Rohde, M. M., Sweet, S. B., Ulrich, C., and Howard, J.: A Transdisciplinary Approach to Characterize Hydrological Controls on Groundwater-Dependent Ecosystem Health, *Frontiers in Environmental Science*, 7, 10.3389/fenvs.2019.00175, 2019.
- Rohde, M. M., Biswas, T., Housman, I. W., Campbell, L. S., Klausmeyer, K. R., and Howard, J. K.: A Machine Learning Approach to Predict Groundwater Levels in California Reveals Ecosystems at Risk, *Frontiers in Earth Science*, 9, 560 10.3389/feart.2021.784499, 2021.
- Rohde, M. M., Stella, J. C., Singer, M. B., Roberts, D. A., Caylor, K. K., and Albano, C. M.: Establishing ecological thresholds and targets for groundwater management, *Nature Water*, 2, 312-323, 10.1038/s44221-024-00221-w, 2024a.
- Rohde, M. M., Albano, C. M., Huggins, X., Klausmeyer, K. R., Morton, C., Sharman, A., Zaveri, E., Saito, L., Freed, Z., Howard, J. K., Job, N., Richter, H., Toderich, K., Rodella, A.-S., Gleeson, T., Huntington, J., Chandanpurkar, H. A., Purdy, 565 A. J., Famiglietti, J. S., Singer, M. B., Roberts, D. A., Caylor, K., and Stella, J. C.: Groundwater-dependent ecosystem map exposes global dryland protection needs, *Nature*, 632, 101-107, 10.1038/s41586-024-07702-8, 2024b.
- Song, M. Y., Li, Z. Q., Xia, D. S., Jin, S., and Zhang, X.: Isotopic evidence for the moisture origin and influencing factors at Urumqi Glacier No.1 in upstream Urumqi River Basin, eastern Tianshan Mountains, *Journal of Mountain Science*, 16, 1802-1815, 10.1007/s11629-018-5348-9, 2019.
- 570 Sun, C. J., Li, W. H., Chen, Y. N., Li, X. G., and Yang, Y. H.: Isotopic and hydrochemical composition of runoff in the Urumqi River, Tianshan Mountains, China, *Environmental Earth Sciences*, 74, 1521-1537, 10.1007/s12665-015-4144-x, 2015.
- Torres-García, M. T., Salinas-Bonillo, M. J., Gázquez-Sánchez, F., Fernández-Cortés, A., Querejeta, J. I., and Cabello, J.: Squandering water in drylands: the water-use strategy of the phreatophyte *Ziziphus lotus* in a groundwater-dependent ecosystem, *American Journal of Botany*, 108, 236-248, 10.1002/ajb2.1606, 2021.
- 575 Vargas, L., Willems, L., and Hein, L.: Assessing the Capacity of Ecosystems to Supply Ecosystem Services Using Remote Sensing and An Ecosystem Accounting Approach, *Environmental Management*, 63, 1-15, 10.1007/s00267-018-1110-x, 2019.
- Wang, P. Y., Li, H. L., Li, Z. Q., Xu, L. P., Yu, F. C., He, J., Dai, Y. P., Zhou, P., Mu, J. X., and Yue, X. Y.: Rapid mass losses of Urumqi River Basin glaciers, eastern Tianshan Mountains revealed from multi-temporal DEMs, 1964-2021, 580 *International Journal of Digital Earth*, 17, 10.1080/17538947.2023.2295990, 2024.
- Wang, Y. N., Kong, X. B., Guo, K., Zhao, C. J., and Zhao, J. T.: Spatiotemporal change in vegetation cover in the Yellow River Basin between 2000 and 2022 and driving forces analysis, *Frontiers in Ecology and Evolution*, 11, 10.3389/fevo.2023.1261210, 2023.



- 585 Xinjiang Institute of Ecology and Geography, C. A. o. S.: Survival in Good order: adaptation strategies of desert plants to drought, 2010.
- Xu, W., Kong, F., Mao, R., Song, J., Sun, H., Wu, Q., Liang, D., and Bai, H.: Identifying and mapping potential groundwater-dependent ecosystems for a semi-arid and semi-humid area in the Weihe River, China, *Journal of Hydrology*, 609, 127789, <https://doi.org/10.1016/j.jhydrol.2022.127789>, 2022a.
- 590 Xu, W. J., Kong, F. H., Mao, R. C., Song, J. X., Sun, H. T., Wu, Q., Liang, D., and Bai, H. F.: Identifying and mapping potential groundwater-dependent ecosystems for a semi-arid and semi-humid area in the Weihe River, China, *Journal of Hydrology*, 609, 10.1016/j.jhydrol.2022.127789, 2022b.
- Yan, X. X., Li, J., Shao, Y., Hu, Z. Q., Yang, Z., Yin, S. Q., and Cui, I.: Driving forces of grassland vegetation changes in Chen Barag Banner, Inner Mongolia, *Giscience & Remote Sensing*, 57, 753-769, 10.1080/15481603.2020.1794395, 2020.
- 595 Yang, X. Y. and Liu, J.: Assessment and Valuation of Groundwater Ecosystem Services: A Case Study of Handan City, China, *Water*, 12, 10.3390/w12051455, 2020.
- Zhang, X. T., Chen, R. S., Liu, G. H., Yang, Y., and Feng, T. W.: Economic value of freshwater provisioning services of the cryosphere in the Urumqi River, Northwest China, *Advances in Climate Change Research*, 12, 894-902, 10.1016/j.accre.2021.09.003, 2021.
- 600 Zurek, A. J., Witzak, S., Dulinski, M., Wachniew, P., Rozanski, K., Kania, J., Postawa, A., Karczewski, J., and Moscicki, W. J.: Quantification of anthropogenic impact on groundwater-dependent terrestrial ecosystem using geochemical and isotope tools combined with 3-D flow and transport modelling, *Hydrology and Earth System Sciences*, 19, 1015-1033, 10.5194/hess-19-1015-2015, 2015.

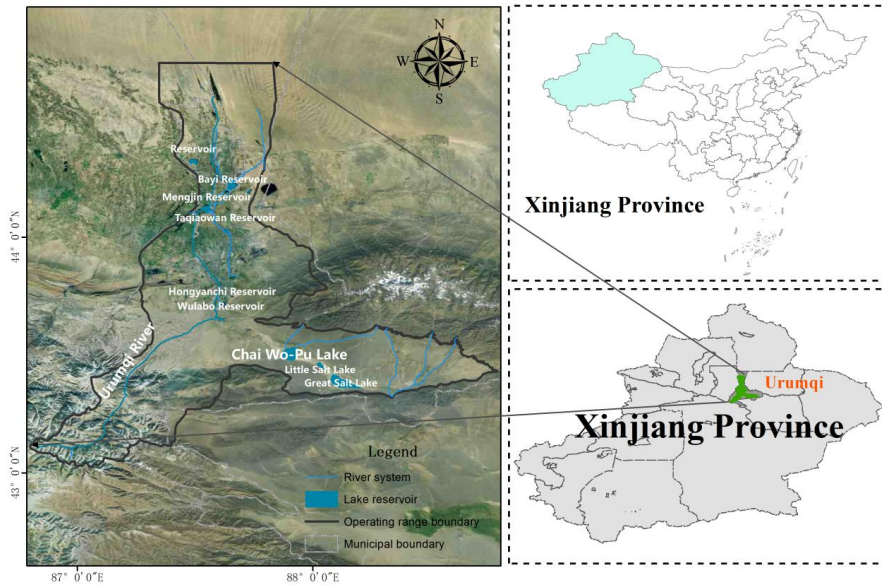


Figure 1: Study area map of the Urumqi River and Chai Wo-pu Basin

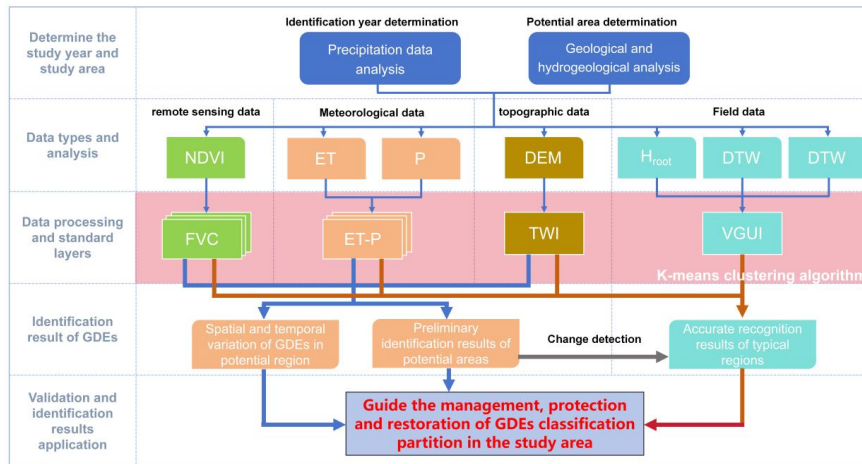


Figure 2: GDEs recognition flow chart

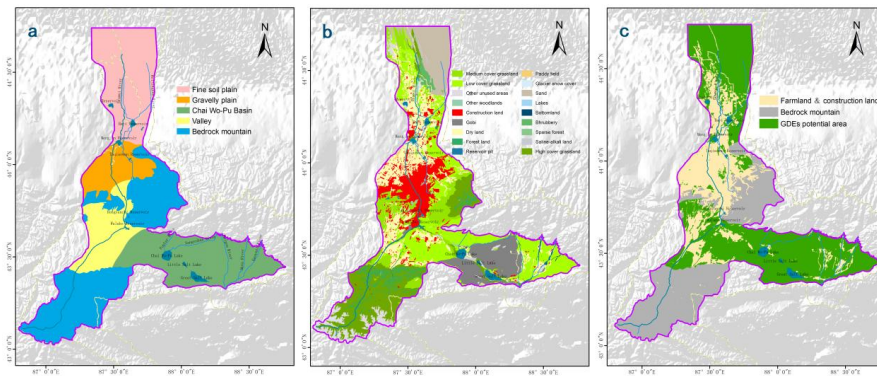


Figure 3: High groundwater correlation areas in the Urumqi River and Chai Wo-pu Basin

(a. Hydrological and geological zoning of the Urumqi River and Chai Wo-pu Basin; b. Land cover types in the Urumqi River and Chai Wo-pu Basin in 2023; c. Potential areas in the Urumqi River and Chai Wo-pu Basin)

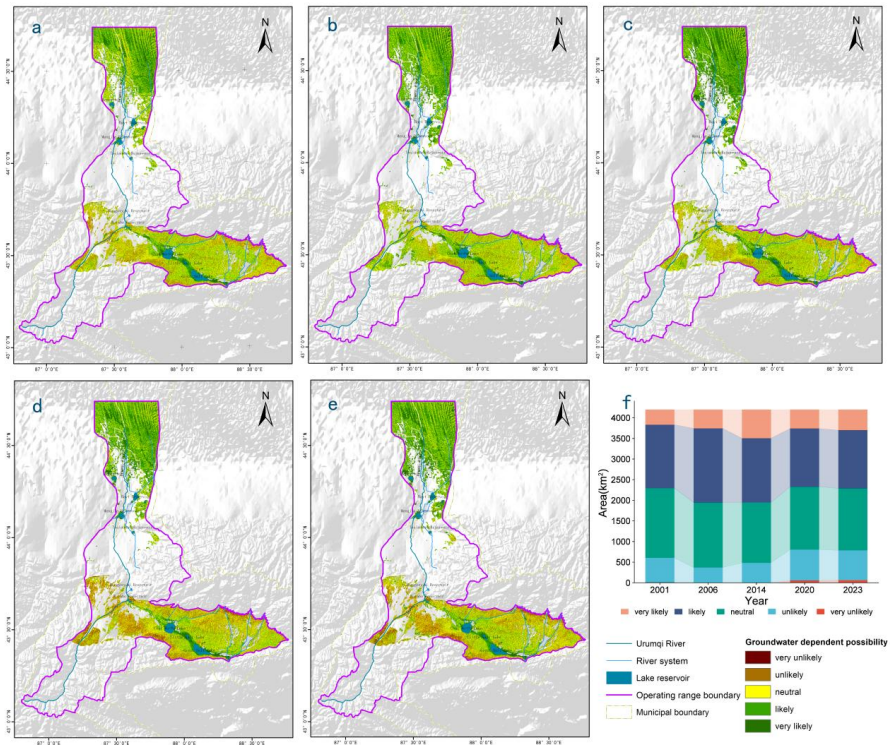


Figure 4: Distribution of GDEs likelihood levels in the Urumqi River and Chai Wo-pu Basin for the years 2001, 2006, 2014, 2020, and 2023

(a. Spatial distribution of GDEs probabilities in 2001; b. Spatial distribution of GDEs probabilities in 2006; c. Spatial distribution of GDEs probabilities in 2014; d. Spatial distribution of GDEs probabilities in 2020; e. Spatial distribution of GDEs possibilities in 2023; f. Changes in the area of GDEs with different probability degrees)

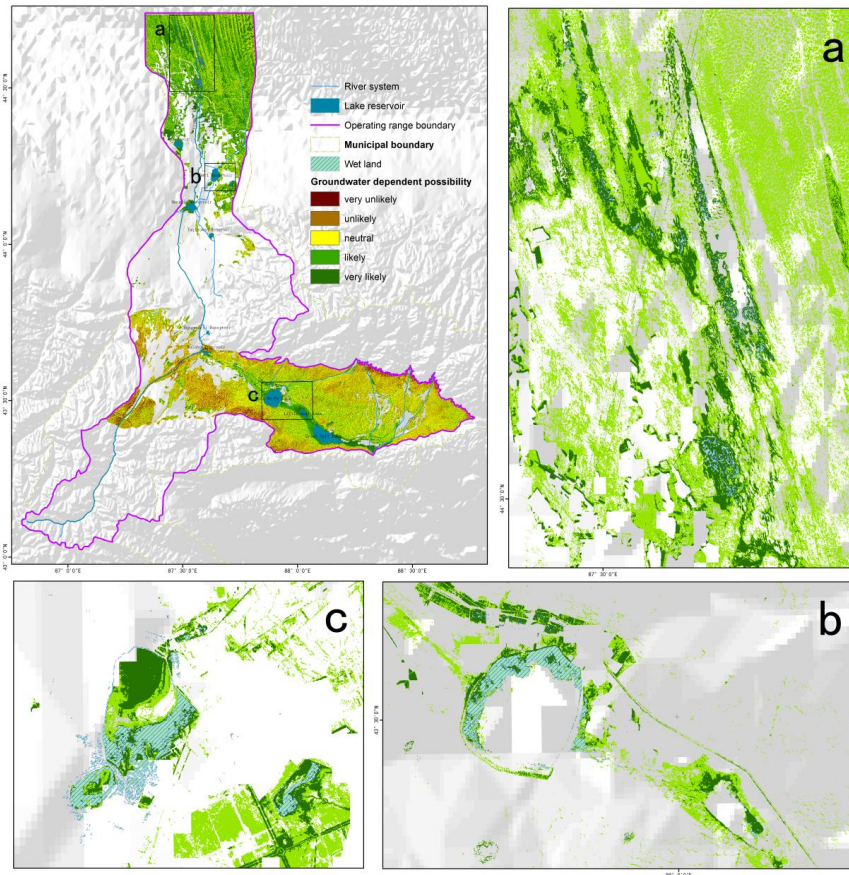


Figure 5: GDEs land cover type (wetland) validation

(a. Dongdao Haizi Area; b. Bayi Reservoir and Petrochemical Wastewater Reservoir Area; c. Chai Wo-pu Lake Area)

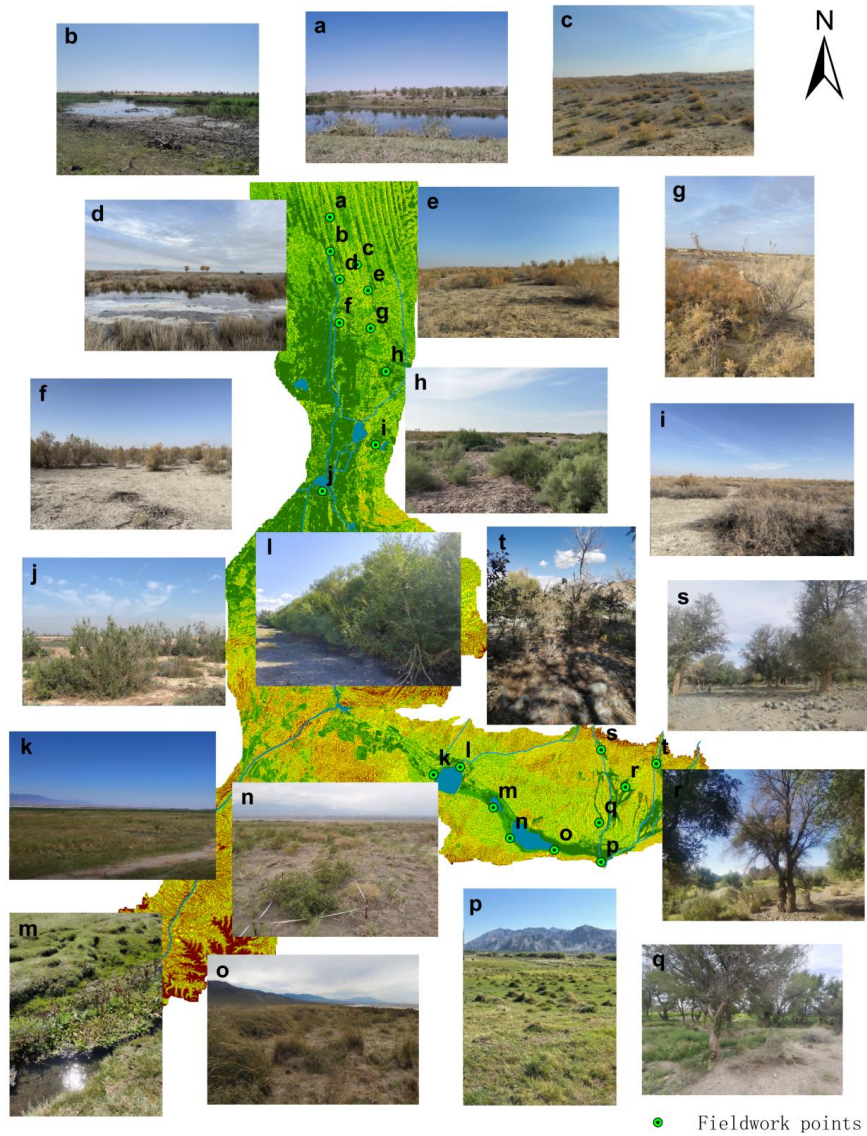


Figure 6: Photos taken at selected validation points
(a-k in Urumqi River basin; l-t in Chaiwopu Basin area)

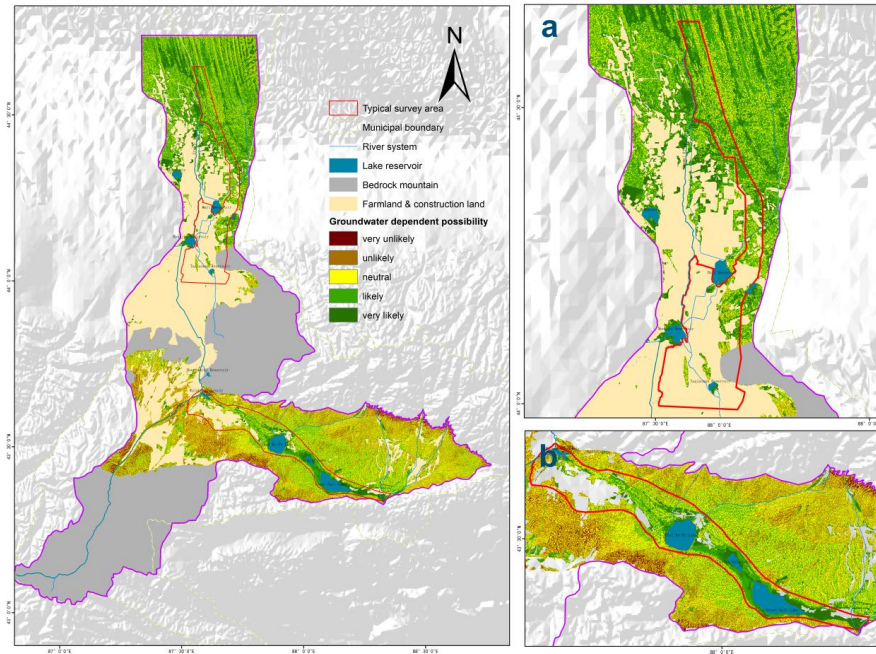


Figure 7: GDEs typical areas in the Urumqi River and Chai Wo-pu Basin
(a. Northern Typical Area; b. Southern Typical Area)

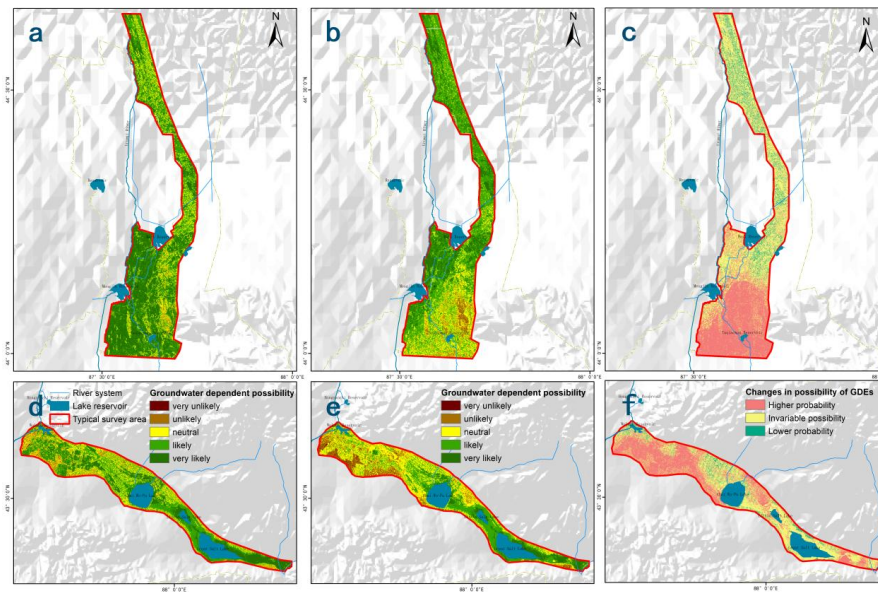


Figure 8: Distribution of GDEs likelihood in the typical areas

(a. Northern Typical Area 3-Indicator GDEs Identification Results; b. Northern Typical Area 4-Indicator GDEs Identification Results; c. Northern Typical Area GDEs Identification Result Change Detection; d. Southern Typical Area 3-Indicator GDEs Identification Results; e. Southern Typical Area 4-Indicator GDEs Identification Results; f. Southern Typical Area GDEs Identification Result Change Detection)



Table 1. Capillary Rise Height for Different Soil types(Li et al., 2014)

Soil types	Capillary Rise Height (m)
Medium-Coarse Sand	0.5
Fine Sand	1.3
Silty Sand	2.0
Sandy Clay	2.6
Clayey Sand	4.2